

# Efficient Data-Driven Model Predictive Control for Demand Response of Commercial Buildings

Marie-Christine Paré, Vasken Dermardiros, and Antoine Lesage-Landry, *Member, IEEE*

**Abstract**—Model predictive control (MPC) has been shown to significantly improve the energy efficiency of buildings while maintaining thermal comfort. Data-driven approaches like neural networks can facilitate system modelling. However, such approaches are generally nonconvex and result in computationally intractable optimization problems. In this work, we design a readily implementable energy management method for small commercial buildings. We then leverage our approach to formulate a real-time demand bidding strategy. We propose a data-driven and mixed-integer convex MPC which is solved via derivative-free optimization given a limited computational time of 5 minutes to respect operational constraints. We consider rooftop unit heating, ventilation, and air conditioning systems with discrete controls to accurately model the operation of most commercial buildings. Our approach uses an input convex recurrent neural network to model the thermal dynamics. We apply our approach to several demand response (DR) settings, including a demand bidding, a time-of-use, and a critical peak rebate program. Controller performance is evaluated on a state-of-the-art building simulation. The proposed approach improves thermal comfort while reducing energy consumption and cost through DR participation, when compared to other data-driven approaches or a set-point controller.

**Index Terms**—Building Energy Management, Demand Response, Input Convex Recurrent Neural Network, Mixed-Integer Programming, Model Predictive Control, Rooftop Unit.

## I. INTRODUCTION

THE built environment stands as one of the most energy-intensive sectors, and as one of the main contributors to climate change. The buildings sector alone accounts for 30% of global energy consumption and contributes to 28% of total greenhouse gas emissions [1]. In the U.S., commercial buildings (CBs) alone consume 46% of the energy used in the building sector. A substantial portion of this energy is allocated to operating their heating, ventilation, and air conditioning (HVAC) systems, which constitute 47% of their total energy consumption [2]. Inefficient HVAC operation, due to the lack of adequate control, often results in significant energy waste [3]. In the U.S., over 90% of CBs fall into the small- to medium-sized category and are predominantly equipped with packaged rooftop units (RTUs). It is estimated that the majority of these buildings still rely on rudimentary controllers, such as ruled-based or set-point (SP)-based [4].

This work was funded by IVADO, Mitacs, and the National Science and Engineering Research Council of Canada (NSERC).

M-C. Paré and A. Lesage-Landry are with the Department of Electrical Engineering, Polytechnique Montreal, MILA & GERAD, Montréal, QC, Canada, H3T 1J4. e-mail: marie-christine.pare@polymtl.ca, antoine.lesage-landry@polymtl.ca

V. Dermardiros is with BrainBox AI, Montréal, QC, Canada, H3A 2L1. e-mail: vdermardiros@gmail.com

Model predictive control (MPC) has demonstrated its ability to improve thermal comfort while achieving energy and cost savings through efficient HVAC operation [3]. Despite extensive research and practical case studies, adoption of the technology within the CBs industry remains limited, primarily due to challenges in automating design, tuning, and implementation. The quality of an MPC solution depends on the model's accuracy and the ability to solve the optimization problem efficiently and globally at its core. Physics-based approaches produce reliable, interpretable models but require significant development effort [5]. In contrast, data-driven approaches promote wide-scale implementation, because they do not require understandings of the system dynamics. This translates into a more transferable approach and lower development costs [3]. Modelling the thermal dynamics of a building can be a challenging task due to their highly nonlinear nature [6]. To address these challenges, many have adopted an approach based on recurrent neural networks (RNNs) because of their high modelling accuracy for dynamic systems [6]. Although RNN-based MPC have been applied to CBs in [7], this results in a nonconvex optimization problem which is computationally intractable. In practice, modelling accuracy is often sacrificed for control tractability, favoring linear models despite their limitations [6].

As part of the largest consumers, CBs can play a significant role in demand response (DR). Their thermal mass provides inherent flexibility, enabling their participation in DR events without compromising thermal comfort. Achieving accurate real-time control of CBs can unlock a large amount of flexibility, thereby enhancing power system resiliency, efficiency, and reliability under high renewable energy penetration, while generating savings for participants [8].

In this work, we design a readily implementable energy management method for demand response of small CBs equipped with RTU-HVAC. Our approach is based on a convex MPC and uses an input convex recurrent neural network (ICRNN) to model the thermal dynamics in a data-driven fashion. We consider discrete controls to accurately model the operation of most RTU-HVAC CBs. We propose a resolution method based on a derivative-free optimization (DFO) solver. The convexity of our approach promotes more efficient computation compared to a conventional RNN-based MPC, as the solver avoids local minima. Then, we formulate a DR strategy where CBs can bid flexibility in a real-time market and present numerical case studies in which various DR programs are discussed, showcasing the full potential of our method. We test our method on a Modelica [9] simulation of a 2-zone CB, a state-of-the-art physics-based simulation.

We now review the related literature on input convex neural networks (NNs) and MPC-based bidding strategy for CBs. Efforts have been made to develop a class of input convex NNs that can be easily embedded in an optimization framework like MPC. First introduced by [10], input convex neural networks (ICNNs) have constraints on their architecture that guarantee the NN's convexity in its inputs, thus permitting efficient global optimization. In [11], the class of convex NNs is extended to include the ICRNN. The authors of [11] also formally prove the representation ability and efficiency of both ICNNs and ICRNNs. In their case studies, a real-time HVAC control experiment is presented on a simulation of a large-scale office building. The ICRNN-based MPC achieves the largest energy reduction when compared to the ones based on a nonconvex RNN or a linear model. In [12], a real-life case study considering an apartment room is presented and shows that an ICNN-based MPC successfully keeps the temperature within the comfort zone most of the time. In [13], the authors of [12] extend their previous work to compare various convex and data-driven MPC approaches, namely a thermal model based on a random forest, a physics-informed ARMAX, and an ICNN. Contrarily to previous work [11]–[13] in this literature stream, we here consider discrete HVAC controls and solve the problem as a mixed-integer optimization problem. We then utilize our approach for several DR applications. Discrete control models promote minimal building upgrades and hence increase its potential for the practical implementation of our method.

MPC-based methods have been leveraged for demand bidding of CBs. In [14], the authors present an experimental demonstration where CBs' HVAC systems are used to provide ancillary frequency regulation services in the Swiss energy market. Participants acquire energy in the day-ahead (DA) market, which serves as a baseline for the following day, and submit flexibility bids accordingly. The baseline and bid quantities are determined by solving a robust optimization problem, and a standard MPC is used to operate HVAC systems and revise bids in the intraday market. In [15], a method for real-time coordination of building consumption and energy scheduling of power systems is proposed. This method utilizes an MPC to plan the operation of HVAC systems and battery energy storage, as well as to generate demand bid curves. In [16], an MPC framework for the DA market enables CBs to submit bids for demand reductions. The control architecture consists of two sequential levels: the first level determines the building's daily participation in the market, and the second level handles real-time operations. These works lack a precise model of the thermal dynamics, as they depend solely on a linear model and are generally tailored to a specific market. We address these limitations by formulating a new adaptable MPC-based bidding strategy utilizing a discrete ICRNN CB model.

Our specific contributions are as follows.

- We present numerical case studies showcasing several DR settings (Sections III-B2–III-B4).
- We formulate a mixed-integer piecewise-linear and data-driven MPC for cooling operations of RTU-based small CBs (Section II-C1).
- We leverage a precise discrete model to formulate an adaptable real-time DR bidding strategy (Section III-B2).

We detail our modelling approach and formulate RTU-HVAC control problems in Section II. In Section III, we present our case studies wherein we assess the performance of our proposed approach, covering inference in Section III-A and control in Section III-B. We conclude in Section IV.

## II. MODELLING AND PROBLEM FORMULATION

We now present the considered building setting, then introduce the thermal dynamics model. We conclude with MPCs for both a base controller and a demand bidding strategy.

### A. System Description

We focus on a small CB served by RTUs, divided into  $n_z \in \mathbb{N}$  zones, where  $n_z$  usually ranges from 1 to 3 [4]. Each zone is equipped with its own thermostat and its associated RTU receiving controls every 5 minutes. A typical RTU comprises  $n_u \in \mathbb{N}$  components, such as electric heating and cooling coils with two intensities each, as well as a fixed-speed fan. Each of these components is controlled using ON/OFF actuation. The reduced control space for cooling operations can be summarized as two intensities of cooling,  $u_{c1} \in \{0, 1\}$  for intensity 1 and  $u_{c2} \in \{0, 1\}$  for intensity 2, and fan ventilation  $u_f \in \{0, 1\}$ . Let  $\mathbf{u}_{\text{RTU}} = [u_{c2}, u_{c1}, u_f]^\top$  be the control variables vector. The set  $\mathcal{U} = \{[0, 0, 0, 0, 0]^\top, [0, 0, 1, 0, 0]^\top, [0, 1, 1, 0, 0]^\top, [1, 1, 1, 0, 0]^\top\}$  is the set of valid reduced controls for one RTU, where  $\mathbf{u}_{\text{RTU}} \in \mathcal{U}$ . For the remainder of this work, we consider the possibility of having more than one RTU, such that the number of controls is  $n_z n_u$ . Let  $\mathbf{u} \in \mathcal{U}^{n_z}$  represent the controls for all  $n_z$  RTUs concatenated together. Let  $\mathbf{p}^c \in \mathbb{R}^{n_z n_u}$  denote the component power rating of the RTUs collected within a vector.

### B. Building Thermal Modelling

We base our approach on the work of [11] to fit a convex and data-driven model of the building's thermal dynamics with an ICRNN. The ICRNN architecture is presented in Figure 1. RNNs are a class of NNs that carry a state to represent the information seen in previous time steps with a memory window length  $w \in \mathbb{N}$ , enabling them to perform accurate multi-step predictions [11], [17]. Let  $\hat{\mathbf{u}}_t = [\mathbf{u}_t, -\mathbf{u}_t]$

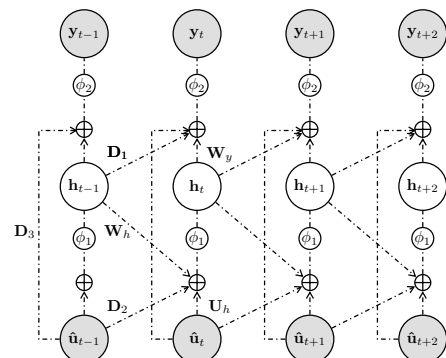


Fig. 1: Architecture of an ICRNN.

represent the extended inputs, and let  $\hat{\mathcal{U}}$  denote the set of extended valid controls. By constraining the architecture of an RNN during training, we can guarantee the convexity of the resulting scalar function with respect to its inputs  $\hat{\mathbf{u}}_t, \forall t$ . As a result, the trained ICRNN can be embedded into an optimization problem which can then be solved efficiently to global optimality. Such NN is described by (1)–(2). In our context, it maps input  $\hat{\mathbf{u}}_t \in \hat{\mathcal{U}}$  to output  $\mathbf{y}_t \in \mathbb{R}^{n_z}$  with hidden state  $\mathbf{h}_t : \hat{\mathcal{U}} \times \mathbb{R}^{n_h} \mapsto \mathbb{R}^{n_h}$ , where  $n_h \in \mathbb{N}$  is the number of hidden units, with the parameters  $\mathbf{U}_h, \mathbf{W}_h, \mathbf{P}_2, \mathbf{b}_h, \mathbf{W}_y, \mathbf{P}_1, \mathbf{P}_3$ , and  $\mathbf{b}_y$ :

$$\mathbf{h}_t = \phi_1(\mathbf{U}_h \hat{\mathbf{u}}_t + \mathbf{W}_h \mathbf{h}_{t-1} + \mathbf{P}_2 \hat{\mathbf{u}}_{t-1} + \mathbf{b}_h) \quad (1)$$

$$\mathbf{y}_t = \phi_2(\mathbf{W}_h \mathbf{h}_t + \mathbf{P}_1 \mathbf{h}_{t-1} + \mathbf{P}_3 \hat{\mathbf{u}}_t + \mathbf{b}_y). \quad (2)$$

The sufficient conditions for the convexity of the network defined by (1)–(2) are that its parameters  $\mathbf{U}_h, \mathbf{W}_h, \mathbf{P}_2, \mathbf{W}_y, \mathbf{P}_1$ , and  $\mathbf{P}_3$  are non-negative and its activation functions  $\phi_1$  and  $\phi_2$  are convex and non-decreasing (e.g., ReLU or LeakyReLU). The resulting trained-NN is convex and non-decreasing over  $\hat{\mathbf{u}}_t$ , but its output can be decreasing or non-decreasing with respect to  $\mathbf{u}_t$ .

### C. Model Predictive Control

We now introduce our control problems. We begin by presenting our base controller, followed by our demand bidding strategy.

1) *Base Controller*: The CB energy management problem is formulated as a rolling horizon optimization problem. The objective is to minimize electrical operational costs, i.e., the cost of energy use and peak demand associated with the RTUs, while maintaining thermal comfort and satisfying equipment requirements over the prediction horizon  $T \in \mathbb{N}$ , in all  $n_z$  zones. For all  $t \in \{1, 2, \dots\}$ , let  $\mathcal{T}_t = \{t, \dots, t+T\}$  be the set of MPC intervals. Let  $\theta^t \in \mathbb{R}^{n_z}$  be the indoor air temperature (IAT), and  $\Delta\theta^t = \theta^t - \theta^{t-1}$  the IAT variations between two sampling steps  $\Delta t > 0$ , in all  $n_z$  zones. The MPC problem is presented in (3)–(9) and described next.

$$\min_{\mathbf{u}^k, k \in \mathcal{T}_t} \sum_{k \in \mathcal{T}_t} \lambda_E^k E^k + \lambda_P \max_{k \in \mathcal{T}_t} \left\{ \mathbf{u}^{k\top} \mathbf{p}^c \right\} \quad (3)$$

$$\text{s.t. } \Delta\theta^k = f_{\text{ICRNN}}(\mathbf{x}^{k-w}, \dots, \mathbf{x}^k), \quad \forall k \in \mathcal{T}_t \quad (4)$$

$$\theta^{k-1} + \Delta\theta^k \leq \bar{\theta}^k, \quad \forall k \in \mathcal{T}_t \quad (5)$$

$$\sum_{\tau=k-\rho}^{k-1} \max\{\mathbf{u}^{\tau-1} - \mathbf{u}^\tau\} \leq 1 - \mathbf{u}^k, \quad \forall k \in \mathcal{T}_t \quad (6)$$

$$E^k = \mathbf{u}^{k\top} \mathbf{p}^c \Delta t, \quad \forall k \in \mathcal{T}_t \quad (7)$$

$$\hat{\mathbf{u}}^k = \begin{bmatrix} \mathbf{u}^k \\ -\mathbf{u}^k \end{bmatrix}, \quad \mathbf{x}^k = \begin{bmatrix} \mathbf{s}^k \\ \hat{\mathbf{u}}^k \end{bmatrix}, \quad \forall k \in \mathcal{T}_t \quad (8)$$

$$\mathbf{u}^k \in \mathcal{U}^{n_z}, \quad \forall k \in \mathcal{T}_t. \quad (9)$$

We consider a time-varying rates for energy  $\lambda_E^t \geq 0$ , and a fixed rate on peak power demand  $\lambda_P \geq 0$ , as utilities usually bill commercial consumers for both. Peak demand fees are based on the maximum power usage observed during a month [18]. Because of the lack of whole building's power profiles due, for example, to submetering, we aim to minimize

the peak demand induced by the RTUs over the prediction horizon as a proxy. Constraints (4)–(5) represent the thermal comfort zone, where  $\bar{\theta}^t \in \mathbb{R}^{n_z}$ ,  $t \in \{1, 2, \dots\}$ , is the upper bound on IAT, for all  $n_z$  zones. The building's thermal dynamics are described by a parametrized ICRNN,  $f_{\text{ICRNN}} : \mathbb{R}^{(2n_u n_z + n_s) \times T} \mapsto \mathbb{R}^{n_z \times T}$  that takes as inputs extended controls  $\hat{\mathbf{u}}^t \in \hat{\mathcal{U}}$ , and the  $n_s \in \mathbb{N}$  building's state variables, i.e., exogenous variables, defined for all  $t \in \{1, 2, \dots\}$ , as  $\mathbf{s}^t \in \mathbb{R}^{n_s}$ . Details about the ICRNN, including its architecture and training procedure, are presented in Section III-A1. We omit the lower bound on IAT  $\theta^t \in \mathbb{R}^{n_z}$ ,  $t \in \{1, 2, \dots\}$ , to maintain convexity as superlevel sets of a convex functions are generally non-convex [12]. This relaxation is not limiting for cooling operations because, by minimizing energy consumption and peak power, the IAT will tend to be close to the upper bound. We plan to extend this approach to heating operations in future work. Constraint (6) prevents equipment toggling, as short cycling significantly decreases the efficiency of units [19]. It ensures that each RTU component remains in the same state during  $\rho \in \mathbb{N}$  time steps when transitioning from ON to OFF. Here,  $\mathbf{0} \in \mathbb{R}^{n_z n_u}$  denotes the zero vector. Constraint (7) represents the energy consumed during a control round. Constraint (8) defines the inputs of the ICRNN, and (9) states the domains of the optimization variables. Considering our ICRNN architecture further described in Section III-A1, the problem (3)–(9) is a mixed-integer piecewise linear optimization problem. When the binary variables are relaxed to continuous ones, its objective function and its feasible set are convex, and the proposed MPC is a convex problem [20]. Convexity of the relaxed optimization problem guarantees that the solver avoids getting stuck in local minima, and therefore promotes higher solution quality with respect to conventional NN-based MPC.

2) *Demand Bidding Strategy*: We now propose a strategy that allows RTU-based CBs participation in a DR program, leveraging an approach that balances modelling accuracy with computational efficiency. Our aim is to enhance bid accuracy and improve the estimation of potential gains. Participants can bid capacity in the real-time market, which operates on 5-minute intervals, matching the CB's operating timescale. Market parameters such as the minimum bid size, the trading intervals time span and gate closure times for bid submission tend to differ in each market [21]. We formulate a model that can be easily adapted to different intraday markets like CAISO, AEMO, and PJM. We draw inspiration from the Frequency Control Ancillary Services (FCAS) market of the Australian National Electricity Market (NEM) requirements for the response speed and duration. FCAS are market-based ancillary services that are used to maintain the grid's frequency to a normal operating point by balancing generation and demand. Frequency control services are further divided into regulation and contingency services. Here, we target contingency delayed-raise and delayed-lower services which require participants to provide an increase or a curtailment of power and maintain it for 5 minutes. When called, participants must respond within 5 minutes. Participants are rewarded based on their availability, regardless of if they are called or not [22]. Finally, we make the following assumptions regarding some

of the market requirements.

- 1) The service is rewarded based on deviations from a baseline of HVAC power data provided by the independent system operator (ISO).
- 2) We adopt a price-taker bidding strategy. This assumption is not too restrictive, as markets like CAISO only allow DR participants to bid as price-takers in the real-time market [23].
- 3) We assume that bids in the day-ahead market have already been submitted if it is a necessary step to participate in the intraday market.
- 4) We omit the minimum-sized bid requirement. If necessary, multiple individual bids can be aggregated.

We now model common market operations to ensure the adaptability and transferability of our approach. We consider the following timeline of events for a given trading interval starting at  $t + 3$ . Participants submit their bids to the ISO before the market's gate closure at market interval  $t$ . Once closed, bid modifications are no longer possible. Then follows the settlement period, during which the ISO receives all bids and secures enough resources. By the end of this period, participants receive a guarantee of payment if their bid is cleared in the market at  $t + 1$ . Subsequently follows a standby period where participants are waiting to receive the DR signal  $\sigma_{-}^{t+3} \in \{0, 1\}$  from the ISO, where  $\sigma_{-}^{t+3}$  represent being called ( $\sigma_{-} = 1$ ) or not ( $\sigma_{-} = 0$ ). Upon its reception at  $t + 2$ , participants are required to fulfill their service bid.

Next, we formulate a real-time bidding strategy for a single CB. We define  $\mathcal{W}_t \subseteq \mathcal{T}_t$  as the set of market intervals closed for bid modifications. Let  $\lambda_{-}^t \geq 0$ ,  $t \in \{1, 2, \dots\}$ , be the market clearing prices (MCPs) for energy curtailment. Let  $c_{-}^t \geq 0$ ,  $t \in \{1, 2, \dots\}$ , be the amount of capacity previously settled by the ISO. Let  $p_{\text{baseline}}^t \geq 0$ ,  $t \in \{1, 2, \dots\}$  be the HVAC power baseline. The MPC for demand bidding is provided in (10)–(13) and discussed next.

$$\min_{\hat{\mathbf{u}}^k, k \in \mathcal{T}_t} \sum_{k \in \mathcal{T}_t} \lambda_{-}^k E_{-}^k - \sum_{k \in \mathcal{T}_t \setminus \mathcal{W}_t} \lambda_{-}^k \Delta E_{-}^k - \sum_{k \in \mathcal{W}_t} \lambda_{-}^k R_{-}^k \quad (10)$$

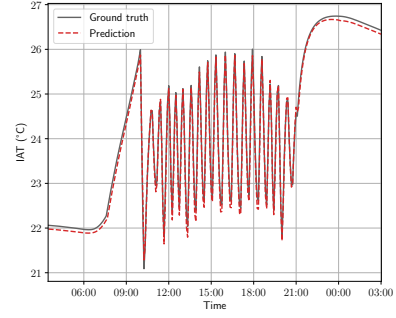
$$\text{s.t.} \quad (4) - (9)$$

$$\Delta E_{-}^k = \left( p_{\text{baseline}}^k - \mathbf{u}^{k \top} \mathbf{p}^c \right) \Delta t, \quad \forall k \in \mathcal{T}_t \setminus \mathcal{W}_t \quad (11)$$

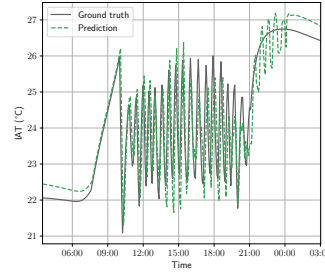
$$p_{\text{baseline}}^k - \mathbf{u}^{k \top} \mathbf{p}^c \geq c_{-}^k, \quad \text{if } \sigma_{-}^k = 1, \quad \forall k \in \mathcal{W}_t \quad (12)$$

$$R_{-}^k = c_{-}^k \sigma_{-}^k, \quad \forall k \in \mathcal{W}_t \quad (13)$$

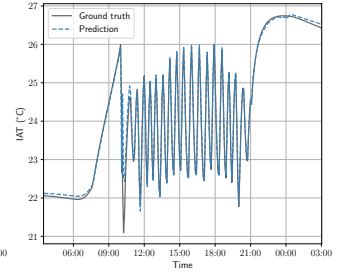
The objective function (10) is defined in terms of the energy cost, a penalty component, and rewards for curtailment services. When the power consumption exceeds the baseline, the penalty term is positive and is proportional to the deviation from the baseline. Conversely, when energy consumption is below the baseline, the penalty term is negative and equal to the reward for the services provided. This formulation is chosen to ensure the problem's convexity and to eliminate the need to introduce equality constraints or supplementary variables. This consideration is especially relevant as the problem is solved through DFO, which will be discussed in Section III. Constraint (11) represents the amount of energy adjustments made with respect to the baseline. Once a bid is cleared in the market, participants are expected to provide the



(a) ICRNN model in zone 2.



(b) Linear model in zone 2.



(c) LSTM model in zone 2.

Fig. 2: Thermal dynamics fitting comparison.

adequate service when called by the ISO. This is modelled by constraint (12). When solving the MPC problem, we assume  $\sigma_{-}^{t+3} = 1$  from the market closure until the end of the bid settlement period. After this period, it is updated to its true value. If our bid is cleared in the market, it remains set to 1 during the standby period until the reception of the true dispatch signal. Finally, constraint (13) defines the rewards.

### III. NUMERICAL CASE STUDIES

In this section, we conduct numerical experiments on a model based on the 2-zone building from the Modelica Buildings Library [9], and use Dymola as the compiler. The library supports multi-zone heat transfer and multi-zone airflow [9]. The power ratings of the RTU components are  $p_{c1} = p_{c2} = 2.272$  kW and  $p_f = 0.637$  kW. The simulated experiments are taking place in Miami from January 1<sup>st</sup>–4<sup>th</sup>, 2021 [24], a period requiring cooling. Given that the control round of each RNN-based MPC has a duration of 5 minutes, we have limited the experiment duration. However, we present results across various DR settings over full days of operations, considering different comfort zones based on occupancy. Specifically, the thermal comfort zone of IAT is set to  $[20^\circ\text{C}, 24^\circ\text{C}]$  during occupancy hours, and to  $[18^\circ\text{C}, 28^\circ\text{C}]$  during unoccupied periods. The simulation environment is employed for data generation for model training, and subsequently for assessing the performance of the controllers. Model accuracy is presented in Section III-A, and then the controller performance is discussed in Section III-B.

#### A. Modelling Accuracy

We now describe the procedure to train the ICRNN and its benchmarks. Results are presented in Section III-A3.

1) *ICRNN*: Our inference approach for multi-step-ahead prediction is based on a multi-output sequence-to-sequence model with a prediction horizon of 2h and a past data horizon of 3h. We use 6 months of data with a 5-minute sampling interval. The dataset is randomly sampled to form training, validation, and testing sets, each comprising 60%, 20%, and 20% of the full dataset size, respectively. Following this, we apply min-max scaling to the data. For feature selection, a correlation analysis is used to target the relevant features and then a forward selection method is applied. The features selected include the extended controls  $\hat{\mathbf{u}}^t$  and the state variables  $\mathbf{s}^t$ . The state variables consist of the outdoor air temperature (OAT), the global horizontal irradiance (GHI), the time of the day and of the week in sin/cos encoding used as representations of the building occupancy. As for the target variables, the ICRNN is used to predict  $\Delta\theta^t$  [12]. Predicting  $\Delta\theta^t$  instead of the IAT leads, in our case, to a higher modelling accuracy. We use a ReLU activation function for  $\phi_1$  and a linear activation function of the output layer  $\phi_2$ . Hyperparameter tuning is performed with `ORION`, a black-box optimization framework [25]. The tuned hyperparameters include the number of hidden units, the number of hidden layers, and the learning rate. Finally, early stopping is implemented to prevent overfitting during training.

2) *Benchmark*: To further investigate the trade-off between modelling accuracy and computational tractability, we use a linear model and a long short-term memory (LSTM) RNN as benchmarks. In this work, the nonconvex MPC serves as a benchmark for model accuracy, but is computationally intractable. The linear MPC acts as a benchmark for computational tractability but with limited modelling abilities. Lastly, the greedy controller represents control simplicity.

a) *Linear*: We use a multi-output first order autoregressive exogenous input (ARX) model and employ a recursive approach for generating multi-step-ahead prediction. Input features include OAT, time of day of week in sin/cos encoding at  $t$ , GHI from  $t-3$  to  $t$ , and  $\Delta\theta^t$  from  $t-4$  to  $t-1$ .

b) *Nonconvex*: We use an LSTM NN. LSTMs have been widely applied to building modelling because of their high accuracy [26]. However, their highly nonlinear structure can potentially lead the solver to converge to a local minimum. We follow the same process for feature selection, training, and hyperparameter tuning as we do for the ICRNN model.

c) *Greedy*: We employ an SP controller that takes decisions based on the current occupancy status and temperature conditions relative to comfort bounds and dead bands.

3) *Results*: We compare our modelling approach with benchmark models. Figure 2 illustrates the prediction performance over a 24-hour period in one of the two zones. To fit the NN models, we employ a recurrent layer of 60 units for the ICRNN and 45 units for the LSTM. We compute the corresponding root mean square error (RMSE) and their standard deviation for each predictive model. In terms of fitting performances, the linear model produces the largest error values with a RMSE of  $(0.45 \pm 0.04)^\circ\text{C}$ . This is primarily due to error propagation over time resulting from the recursive approach and its limitation in capturing nonlinear patterns, such as coupling between zones and thermal inertia. The

TABLE I: Controller comparison for the flat-rate pricing.

| Metrics                              | Day 1 | Day 2 | Day 3 |
|--------------------------------------|-------|-------|-------|
| <b>Greedy</b>                        |       |       |       |
| Avg. discomfort [ $^\circ\text{C}$ ] | 0.307 | 0.360 | 0.437 |
| Energy [kWh]                         | 52.39 | 52.73 | 50.32 |
| Toggling                             | 0     | 0     | 0     |
| <b>Linear</b>                        |       |       |       |
| Avg. discomfort [ $^\circ\text{C}$ ] | 0.015 | 0.014 | 0.052 |
| Energy [kWh]                         | 95.03 | 93.40 | 94.16 |
| Toggling                             | 0     | 0     | 0     |
| <b>Convex</b>                        |       |       |       |
| Avg. discomfort [ $^\circ\text{C}$ ] | 0.069 | 0.005 | 0.066 |
| Energy [kWh]                         | 52.63 | 60.12 | 30.32 |
| Toggling                             | 0     | 0     | 0     |
| <b>Nonconvex</b>                     |       |       |       |
| Avg. discomfort [ $^\circ\text{C}$ ] | 0.003 | 0.005 | 0.006 |
| Energy [kWh]                         | 59.98 | 67.11 | 62.37 |
| Toggling                             | 0     | 0     | 0     |

LSTM model, conversely, shows the lowest error values with a RMSE of  $(0.09 \pm 0.01)^\circ\text{C}$ . An LSTM NN has a memory cell that can capture information from earlier time steps and store it for later use, which helps addressing the problem of vanishing or exploding gradient [17], thereby contributing to a more accurate representation of thermal inertia. Our ICRNN model shows significant improvements when compared to the linear model with a RMSE of  $(0.14 \pm 0.03)^\circ\text{C}$ . Because the ICRNN is a piecewise linear convex approximation, it has representation limitations. It remains a competitive alternative to the LSTM.

## B. Controller Performance

We now assess the performance of the controllers under different pricing mechanisms and DR programs.

In our control experiments, we introduce Gaussian noise to simulate uncertainty in time-varying data and compute standard deviations from historical data. Specifically, we apply noise to the OAT and the GHI. To ensure a reasonable variation over a 2-hour horizon, the standard deviations are scaled down by a factor of 10 for IAT and 50 for GHI, and the amount of noise is increased linearly across the prediction horizon. In Section III-B2, the same process is applied to introduce noise in energy prices and MCPs, with standard deviations adjusted by a factor of 10. As for the performance metrics, we evaluate thermal discomfort, defined at time step  $t$  as  $\mathbf{1}^\top ([\theta^t - \bar{\theta}^t]^+ + [\theta^t - \bar{\theta}^t]^-) \Delta t$ , where  $\mathbf{1} \in \mathbb{R}^{n_z}$  is the one vector, and toggling based on the satisfaction of constraint (6).

In terms of resolution methods, the MPC based on the linear model is solved with `MOSEK` [27], which returns the global optimum. In case of infeasibility, thermal comfort bounds are relaxed. The NN-based MPCs are solved with the blackbox optimization software `NOMAD` [28] using the `Mesh Adaptive Direct Search` [29] algorithm, which allows for discrete-DFO [30]. For the nonconvex MPC specifically, a `Variable Neighborhood Search` [31] metaheuristic is added to try to escape local minima. In this optimization framework, all constraints, i.e., constraints (4)–(6) and (12) are handled by the `Progressive Barrier` approach, which allows constraint violations. In case of infeasibility, `NOMAD` yields the solution that minimizes the sum of squares of the violations.

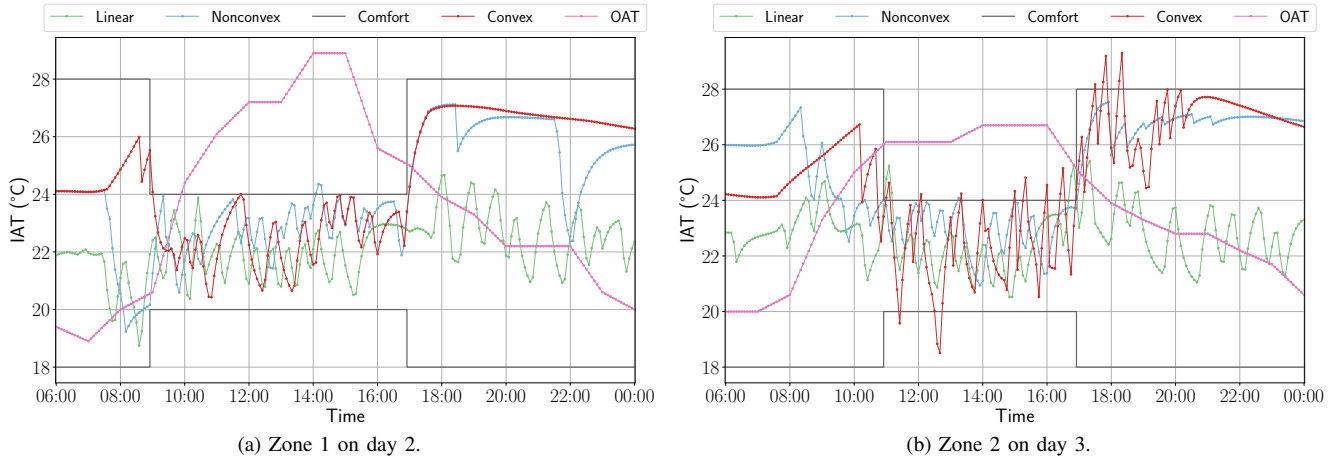


Fig. 3: Controller comparison: IAT profiles during 2 simulated days under a flat-rate pricing.

To initiate the optimization process, the solver requires an initial point. This enables us to leverage the previous solution in a rolling horizon strategy, to effectively guide the new search. To reduce the search space, binary controls presented in Section II-A are converted into integer variables.

1) *Flat-Rate Pricing*: We conducted a 3-day experiment implementing the MPC problem described in (3)–(9), considering both time-invariant energy and power pricing. The energy rate is set to \$0.05303/kWh, and the peak power rate to \$14.58/kW, similarly to [18]. Results for all zones combined are presented in Table I.

In a cooling experiment, the greedy controller toggles around the upper bound on thermal comfort. It thus acts as a more stringent benchmark for energy consumption but induces a significant amount of thermal discomfort. As shown in Table I, on both day 1 and day 3, the greedy controller consumes either the same amount or more energy than the convex MPC, while also causing significant thermal discomfort. These results highlight the importance of operating RTU-HVAC efficiently. With the linear MPC, the controller tends to inefficiently overcool the system, leading to a high energy consumption. This underscores the crucial role of model design in control methods like MPC, as an inadequate model will lead to poor controller performance. Considering the convex approach, the ICRNN has a higher prediction error than the LSTM. In control, prediction errors may lead the IAT outside the thermal comfort zone, as presented in Figure 3. Although the convex MPC problem has only an upper bound on thermal comfort, the IAT is kept within the comfort zones most of the time, as shown in Figure 3(b). In all instances, all controllers avoid toggling of equipment. However, none of them manage to reduce the power peak consumption of 10.37 kW. Given the small number of zones and the experiments taking place during hot days, it may not be feasible to achieve such reduction. Overall, when compared to the more commonly implemented control method, viz., the greedy controller, the convex MPC is the only approach that reduces both energy consumption and discomfort, with respective averages of 8.42% and 86.95% across all simulation days.

TABLE II: Controller comparison for DR programs.

| Demand bidding       |              |                       |          |               |               |
|----------------------|--------------|-----------------------|----------|---------------|---------------|
| Controller           | Energy [kWh] | Avg. dis-comfort [°C] | Toggling | Net cost [\$] | Savings [%]   |
| Greedy               | 52.39        | 0.307                 | 0        | 1.28          | -             |
| Linear               | 82.55        | 0.010                 | 0        | 1.76          | 0.76          |
| Convex               | 45.62        | 0.092                 | 2        | 0.95          | 22.02         |
| Nonconvex            | 52.44        | 0.029                 | 2        | 1.12          | 17.07         |
| Time-of-use          |              |                       |          |               |               |
| Controller           | Energy [kWh] | Avg. dis-comfort [°C] | Toggling | Net cost [\$] |               |
| Greedy               | 52.39        | 0.307                 | 0.0      | 7.82          | -             |
| Linear               | 93.14        | 0.016                 | 0.0      | 12.69         | -             |
| Convex               | 52.29        | 0.033                 | 1.0      | 8.115         | -             |
| Nonconvex            | 61.49        | 0.000                 | 0.0      | 9.53          | -             |
| Critical peak rebate |              |                       |          |               |               |
| Controller           | Energy [kWh] | Avg. dis-comfort [°C] | Toggling | Net cost [\$] | Savings [kWh] |
| Greedy               | 52.39        | 0.309                 | 0        | -0.31         | 7.80          |
| Linear               | 86.79        | 0.060                 | 0        | 3.53          | 5.57          |
| Convex               | 51.70        | 0.054                 | 0        | -0.10         | 7.33          |
| Nonconvex            | 60.04        | 0.002                 | 1        | 3.18          | 2.51          |

2) *Demand Bidding*: We now implement the demand bidding strategy presented in Section II-C2. In this experiment, a common baseline consumption is set for all MPCs, and is established by averaging historical data of the corresponding day of the week. The market's gate closure time is set to 15 minutes before the start of a trading interval. The ISO's decision  $\sigma_-^t$ ,  $t \in \{1, 2, \dots\}$ , on whether to call a service or not is modelled by independent and identically distributed Bernoulli random variables. We assume a probability of 0.9 of being cleared in the market, as we participate as a price-taker, and a probability of being called of 0.4. Real-time energy prices and MCPs are retrieved from [32], [33]. Savings from participation are calculated with respect to a benchmark for each thermal model, obtained by solving the control problem defined by (4)–(10) with  $\lambda_-^t = 0 \forall t$ , and real-time energy prices are used for  $\lambda_E^t$ .

In this experiment, the CB participates in the real-time market by submitting bids over a 24-hour period. Detailed results for all zones combined are presented in Table II. The convex MPC attains the lowest energy consumption and net cost among all controllers. As for the average thermal



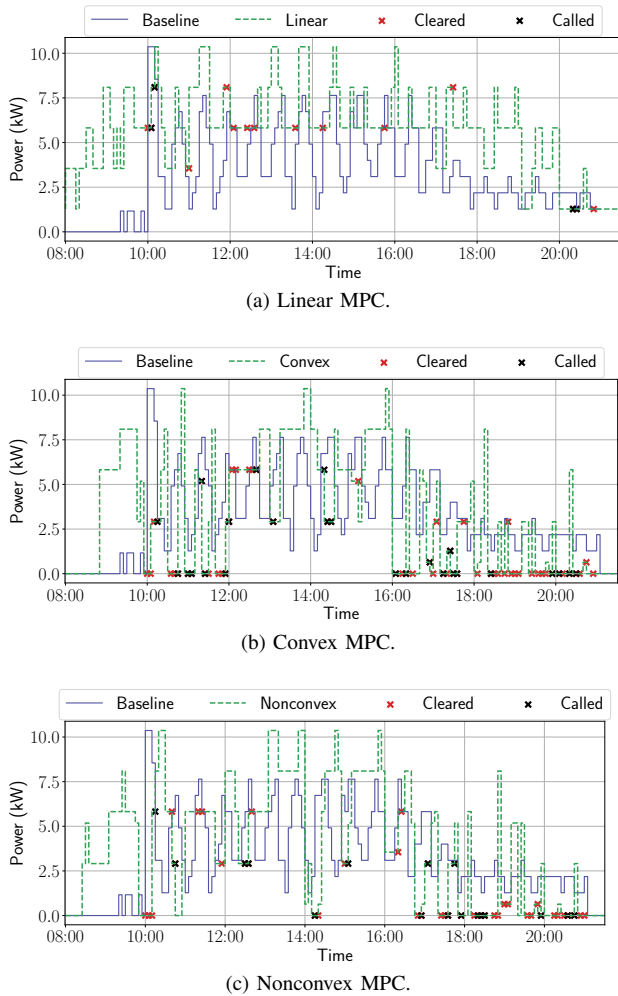


Fig. 4: Power profiles for the demand bidding program.

discomfort, the proposed approach achieves a reduction of 70.03% compared to the greedy approach. Both the convex and nonconvex MPCs show a comparable amount of toggling. In general, a tolerable level of cycling is acceptable, and this remains within reasonable limits, as the results presented include all components of the two RTUs. Regarding savings, the convex approach achieves the largest amount of savings. This can be attributed to the fact that the convex MPC submits significantly more bids into the market, as presented in Figure 4. The convex approach bids 12.35 kWh through 66 individual bids, and is called 28 times. In contrast, the linear MPC submits 2.72 kWh through 16 bids, and the nonconvex submits 7.07 kWh through 47 bids. Finally, the convex approach ends up providing more flexibility to the grid, delivering 4.13 kWh of service, compared to 2.49 kWh for the nonconvex and 1.33 kWh for the linear. During the experiment, all controllers successfully fulfilled their bids. In a real market context, participants who fail to do so could incur a substantial penalty. If feasibility is a concern, constraint (12) could be treated with this *Extreme Barrier* [29] approach to forbid violations.

3) *Time-of-Use*: We now consider a time-of-use (TOU) program, where rates and schedules are based on [34] for the

summer period.

Results for a 24-hour experiment are presented in Table II, and include all zones combined. In this experiment, the convex controller attains the lowest energy consumption among all controllers. While it ranks second in terms of net cost, with a net cost 3.77% higher than the greedy controller, it mitigates discomfort by 89.25% with an equivalent energy usage.

4) *Critical Peak Rebate*: We now consider a critical peak rebate (CPR) program. CPR is a program in which participants receive discounts on their electricity bills in exchange for reducing their demand during critical peak periods. The program utilizes a participant baseline to determine the payment settlement. From the consumer's perspective, CPR is a voluntary and self-controlled initiative that incurs no penalties and requires minimal equipment [35].

In this experiment, the MPC problem is defined by the set (4)–(9), and (11), with objective (10) where the reward term is not included. The electricity rate is structured with a base rate of \$0.076/kWh and a reward of \$0.55/kWh for each kWh reduced from the participant's baseline [36]. The baseline is defined as in Section III-B2. We consider events that take place during the summer, where peak demand typically occurs within the 12:00 PM to 6:00 PM window. To prepare for the event, program participants are assumed to be notified at least two hours in advance.

In Table II, the results of all controllers are compared. The convex approach achieves the lowest energy consumption compared to other controllers without leading to equipment toggling. In terms of net cost, when compared to the greedy controller, it incurs an additional cost of \$0.21, but achieves a reduction of 82.52% in terms of discomfort. In terms of energy savings, the convex approach is able to curtail 7.33 kWh from the baseline, which is only 6.02% less than the greedy controller.

### C. Solution Quality

We now assess the quality of the solution obtained during a 5-minute control horizon imposed by the CB's timescale. During a 24-hour control experiment, we run the convex MPC implemented in Section III-B1. For 30% of the iterations, we run the solver for 5, 10, and 30 minutes. We find that in 92.4% of the instances, the same solution was found with a computation time of 5 minutes as in 10 minutes, and in

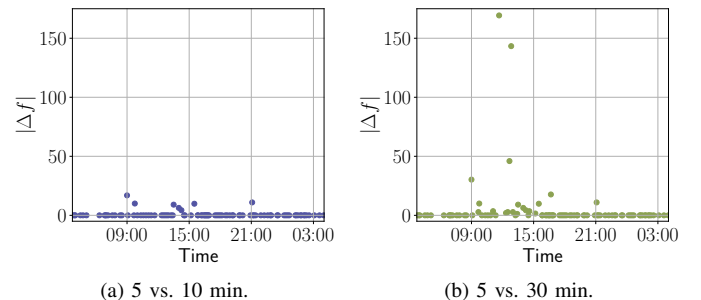


Fig. 5: Comparison of objective function values based on computation time.

78.3% when compared to a computation time of 30 minutes. Figure 5 illustrates the absolute gap between the objective function values,  $|\Delta f|$ . To contextualize these results, large gaps can be attributed to variations in peak power between solutions, as peak power demand is strongly penalized by a rate of \$14.58/kW. However, it's important to note that the objective function values do not reflect real operational costs. This is because we optimize peak power over the MPC horizon rather than considering the observed monthly peak.

#### IV. CONCLUSION

In this work, we propose an energy management method for RTU-HVAC of small CBs. Our convex MPC approach leverages a discrete and data-driven model of the thermal dynamics, making the implementation in RTU-based CBs straightforward. We develop a bidding strategy for the real-time market and apply our approach to a TOU and a CPR program. The performance of the proposed controller is evaluated through a numerical building simulation, and has demonstrated a good compromise between thermal comfort, energy reduction, and cost. In future work, we will extend our approach to an aggregation of small CBs or to a large CB through a decentralized optimization method. We also plan to propose a resolution method that produces provably optimal solutions.

#### REFERENCES

- [1] M. González-Torres, L. Pérez-Lombard *et al.*, "A review on buildings energy information: Trends, end-uses, fuels and drivers," *Energy Reports*, vol. 8, pp. 626–637, 2022.
- [2] A. Allouhi, Y. El Fouih, T. Kousksou *et al.*, "Energy consumption and efficiency in buildings: current status and future trends," *Journal of Cleaner Production*, vol. 109, pp. 118–130, 2015.
- [3] Z. Afroz, G. Shafiqullah, T. Urmee, and G. Higgins, "Modeling techniques used in building HVAC control systems: A review," *Renewable and Sustainable Energy Reviews*, vol. 83, pp. 64–84, 2018.
- [4] S. Katipamula, R. M. Underhill, J. K. Goddard *et al.*, "Small- and medium-sized commercial building monitoring and controls needs: a scoping study," U.S. Department of Energy, Technical Report PNNL-22169 BT0302000, 2012.
- [5] J. Drgoña, J. Arroyo, I. Cupeiro Figueroa *et al.*, "All you need to know about model predictive control for buildings," *Annual Reviews in Control*, vol. 50, pp. 190–232, 2020.
- [6] Z. Wang and Y. Chen, "Data-driven modeling of building thermal dynamics: methodology and state of the art," *Energy and Buildings*, vol. 203, p. 109405, 2019.
- [7] F. Mubaa, K.-K. Nguyen, V. Dermardiros *et al.*, "Context-aware model predictive control framework for multi-zone buildings," *Journal of Building Engineering*, vol. 42, p. 102340, 2021.
- [8] H. Tang, S. Wang, and H. Li, "Flexibility categorization, sources, capabilities and technologies for energy-flexible and grid-responsive buildings: State-of-the-art and future perspective," *Energy*, vol. 219, p. 119598, 2021.
- [9] M. Wetter, W. Zuo, T. S. Nouidui, and X. Pang, "Modelica Buildings library," *Journal of Building Performance Simulation*, vol. 7, no. 4, pp. 253–270, 2014.
- [10] B. Amos, L. Xu, and J. Z. Kolter, "Input convex neural networks," in *Proceedings of the 34th International Conference on Machine Learning*, ser. Proceedings of Machine Learning Research, vol. 70. PMLR, 2017, pp. 146–155.
- [11] Y. Chen, Y. Shi, and B. Zhang, "Optimal control via neural networks: A convex approach," 2019, arXiv:1805.11835.
- [12] F. Büning, A. Schalbetter, A. Aboudonia *et al.*, "Input convex neural networks for building MPC," in *Proceedings of the 3rd Conference on Learning for Dynamics and Control*, ser. Proceedings of Machine Learning Research, vol. 144. PMLR, 07 – 08 June 2021, pp. 251–262.
- [13] F. Büning *et al.*, "Physics-informed linear regression is competitive with two machine learning methods in residential building MPC," *Applied Energy*, vol. 310, p. 118491, 2022.
- [14] T. T. Gorecki, L. Fabietti *et al.*, "Experimental demonstration of buildings providing frequency regulation services in the Swiss market," *Energy and Buildings*, vol. 144, pp. 229–240, 2017.
- [15] T. Wei, Q. Zhu, and N. Yu, "Proactive demand participation of smart buildings in smart grid," *IEEE Transactions on Computers*, vol. 65, no. 5, pp. 1392–1406, 2016.
- [16] C. N. J. Faran A. Qureshi, Tomasz T. Gorecki, "Model predictive control for market-based demand response participation," *IFAC Proceedings Volumes*, vol. 47, no. 3, pp. 11 153–11 158, 2014.
- [17] C. Fan, J. Wang, W. Gang, and S. Li, "Assessment of deep recurrent neural network-based strategies for short-term building energy predictions," *Applied Energy*, vol. 236, pp. 700–710, 2019.
- [18] Hydro-Québec. (2023) Rate M. Accessed: 2023-11-30. [Online]. Available: <https://www.hydroquebec.com/business/customer-space/rates/rate-m-general-rate-medium-power-customers-billing.html>
- [19] W. Kim, S. Katipamula, and R. Lutes, "Improving HVAC operational efficiency in small-and medium-size commercial buildings," *Building and Environment*, vol. 120, pp. 64–76, 2017.
- [20] S. Boyd and V. Lieven, *Convex Optimization*. Cambridge, UK: Cambridge University Press, 2004.
- [21] I. Pavić, M. Beus *et al.*, "Electricity markets overview — market participation possibilities for renewable and distributed energy resources," in *2017 14th International Conference on the European Energy Market (EEM)*, 2017, pp. 1–5.
- [22] Australian Energy Market Operator (AEMO). (2021) Guide to ancillary services in the national electricity market. Accessed: 2022-09-01. [Online]. Available: [https://aemo.com.au/-/media/files/electricity/nem/security\\_and\\_reliability/ancillary\\_services/guide-to-ancillary-services-in-the-national-electricity-market.pdf](https://aemo.com.au/-/media/files/electricity/nem/security_and_reliability/ancillary_services/guide-to-ancillary-services-in-the-national-electricity-market.pdf)
- [23] M. Kohansal and H. Mohsenian-Rad, "A closer look at demand bids in California ISO energy market," *IEEE Transactions on Power Systems*, vol. 31, no. 4, pp. 3330–3331, 2016.
- [24] Building Technologies Office, U.S. Department of Energy. (2023) Energyplus weather (EPW) data. Accessed: 2023-11-30. [Online]. Available: [https://energyplus.net/weather-location/north\\_and\\_central\\_america\\_wmo\\_region\\_4/USA/FL/USA\\_FL\\_Miami.Intl.AP.722020\\_TMY3](https://energyplus.net/weather-location/north_and_central_america_wmo_region_4/USA/FL/USA_FL_Miami.Intl.AP.722020_TMY3)
- [25] X. Bouthillier *et al.* (2023) Epistimo/orion: Asynchronous Distributed Hyperparameter Optimization (v0.2.7). Accessed: 2022-09-01. [Online]. Available: <https://doi.org/10.5281/zenodo.3478592>
- [26] B.-K. Jeon and E.-J. Kim, "LSTM-based model predictive control for optimal temperature set-point planning," *Sustainability*, vol. 13, no. 2, 2021.
- [27] M. ApS, *The MOSEK optimization toolbox for MATLAB manual. Version 9.0.*, 2019. [Online]. Available: <http://docs.mosek.com/9.0/toolbox/index.html>
- [28] S. Le Digabel, "Algorithm 909: NOMAD: Nonlinear optimization with the MADs algorithm," *ACM Transactions on Mathematical Software*, vol. 37, no. 4, pp. 1–15, 2011.
- [29] C. Audet and J. E. Dennis, "Mesh adaptive direct search algorithms for constrained optimization," *SIAM Journal on Optimization*, vol. 17, no. 1, pp. 188–217, 2006.
- [30] C. Audet, S. Le Digabel, and C. Tribes, "The mesh adaptive direct search algorithm for granular and discrete variables," *SIAM Journal on Optimization*, vol. 29, no. 2, pp. 1164–1189, 2019.
- [31] A. C. B. V., and L. S., "Nonsmooth optimization through mesh adaptive direct search and variable neighborhood search," *Journal of Global Optimization*, vol. 41, no. 2, p. 299–318, 2008.
- [32] PJM. (2023) Data Miner 2: Real-time hourly LMPs. Accessed: 2023-11-12. [Online]. Available: [https://dataminer2.pjm.com/feed/rt\\_hrl\\_lmps/definition](https://dataminer2.pjm.com/feed/rt_hrl_lmps/definition)
- [33] ——. (2023) Data Miner 2: Real-time ancillary service market results. Accessed: 2023-11-12. [Online]. Available: [https://dataminer2.pjm.com/feed/reserve\\_market\\_results/definition](https://dataminer2.pjm.com/feed/reserve_market_results/definition)
- [34] Managing costs with Time-of-Use rates. (2023) Ontario Energy Board (OEB). Accessed: 2023-11-30. [Online]. Available: <https://www.oeb.ca/consumer-information-and-protection/electricity-rates/managing-costs-time-use-rates>
- [35] H. Yang, X. Zhang, Y. Ma, and D. Zhang, "Critical peak rebate strategy and application to demand response," *Protection and Control of Modern Power Systems*, vol. 6, no. 1, pp. 1–14, 2021.
- [36] Hydro-Québec. (2023) Rate Flex D. Accessed: 2023-11-30. [Online]. Available: <https://www.hydroquebec.com/residential/customer-space/rates/rate-flex-d-billing.html>